

Axisymmetric Slip Flow of a Powell - Eyring Fluid Due to Induced Magnetic Field

Subba Rao, M. V. ^{*1}, Gangadhar, K. ², and Varma, P. L. N. ¹

¹*Department of Sciences & Humanities, Vignan's Foundation for Science, Technology and Research, Vadlamudi, Andhra Pradesh - 522213, India*

²*Department of Mathematics, Acharya Nagarjuna University, Ongole, Andhra Pradesh - 523001, India*

E-mail: subbaraovu@rediffmail.com

** Corresponding author*

Received: 13 January 2018

Accepted: 27 October 2019

ABSTRACT

The principal aim of this investigation is to study the heat transfer in axisymmetric slip flow of a MHD Powell-Eyring fluid over a radially stretching surface. The mathematical model of the physical problem solved numerically through SRM, SOR and Matlab in-built boundary value problem solver bvp4c. Results are validated by comparing with the results of the earlier studies. It shows that the proposed technique is an efficient numerical algorithm with assured convergence which serves as an alternative to common numerical methods for solving non linear boundary value problems. There is significant improvement in the rate of convergence in conjunction with SOR. The present SRM results compared with the previously published results of homotopy analysis method (HAM) and fourth order Runge-Kutta(RK) Method. Velocity and temperature profiles of the flow for various values of governing physical and fluid parameters are obtained and also the coefficient of skin friction and the local Nusselt number are calculated for the same values of the

parameters. Main findings are: there is a decrease in the velocity and temperature by increasing corresponding slip parameters and the rate of skin friction increases with ϵ and decreases with δ .

Keywords: Spectral relaxation method (SRM), radially stretching surface, Powell - Eyring fluid, slip flow.

1. Introduction

It is clear that most of the industrial and geophysical fluids are non-Newtonian. This led to a study of the boundary layer flow of viscoelastic fluid. Later this proved that a stretching surface and assuming stretching surface velocity is progressively proportional to a fixed origin in terms to its distance. Due to this there are many industrial applications as such production of glass-fiber, in adhesive tapes fabrication, expansion of plastic sheets, metal spinning and in paper films drawing. McCormack and Crane (1973) has been notified that boundary layer flow over a stretching of an elastic flat sheet in their study. Bilal Ashraf et al. (2015) observed the three dimensional boundary layer flow of Eyrng-Powell nanofluid by convectively heated exponentially stretching sheet. Javed et al. (2013) analyzed the boundary layer flow of an Eyring-Powell non-Newtonian fluid over a stretching sheet. Recently, Hayat et al. (2016) considered the study of effect of magnetic hydro dynamics (MHD) boundary layer flow of Powell-Eyring nanofluid over a non-linear stretching sheet with variable thickness. All of the authors mentioned above, continued their investigations by assuming that boundary layer problems with no slip condition. The non-adherence of the fluid to solid boundary is called velocity slip this information is pointed out based on certain circumstances (Yoshimura and Prudhomme (1998)). The impact of slip condition is very useful in technological applications. To include slip condition many studies were conducted. Mansur et al. (2014) investigates the heat transfer and partial slip flow by analyzing nanofluid past stretching sheet.

Jaina and Choudhary (2015) analyzed the MHD effect on boundary layer flow over an exponentially stretching sheet is embedded in a porous medium with slip condition. Shaw et al. (2016) studied that the boundary layer flow over a stretching surface of non-linear convection in nanofluid flow with slip condition. Khalil-Ur-Rehman et al. (2017a) studied the effects of Joule heating, thermal radiations and heat generation on Eyring-Powell fluid flow over a stretching surface. The numerical investigation for MHD thermal and solutal stratified stagnation point flow of Powell - Eyring fluid past a cylindrical

surface was studied by Khalil-Ur-Rehman et al. (2017b). Khalil-Ur-Rehman et al. (2017c) investigated the MHD mixed convection flow of Eyring -Powell fluid over an inclined cylindrical stretching surface. Khalil-Ur-Rehman et al. (2017d) studied the heat and mass transfer mechanisms for Powell - Eyring fluid using Lie group analysis. Khalil-Ur-Rehman et al. (2018) numerically investigated the Prandtl - Eyring fluid model with both heat and mass transfer using scaling group of transformations.

In the literature there are very few authors who have studied about axisymmetric slip flow of Powell-Eyring fluid over a radially stretching surface by considering into an account the impact of transverse magnetic field using SRM. The principal aim of the investigation is to examine the characteristics of heat transfer in a Powell-Eyring fluid driven by a radially impermeable stretching surface in presence of slip, transverse magnetic field using spectral relaxation method. Recently, Ismail et al. (2019) explored the analysis of flow and heat transfer over an exponentially shrinking sheet in presence of heat generation.

2. Physical Model and Mathematical Formulation

Let us consider the two-directional axisymmetric slip flow of a Powell-Eyring fluid. Because of radially stretching sheet which is located at $z = 0$ fluid gets motion, while the fluid occupying area is $z \geq 0$. A non-uniform magnetic field $B(r) = B_0 r$ is imposed transverse to the stretching sheet. Here chosen magnetic Reynolds number is small and induced magnetic and electric fields are not considered into an account, where $T_w > T_\infty$. Physical model under consideration is shown in Figure 1.

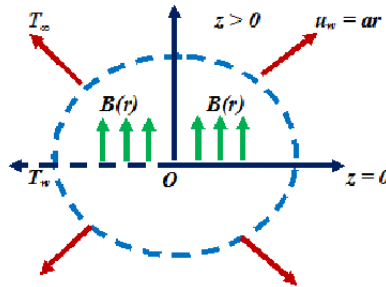


Figure 1: Schematic diagram .

The Powell-Eyring fluid model is satisfied by Cauchy stress tensor, is given as in the form

$$T = -\rho I + \tau. \tag{1}$$

For the Powell-Eyring fluid yielding τ_{ij} is given as below

$$\tau_{ij} = \mu \frac{\partial u_i}{\partial x_j} + \frac{1}{\beta} \arcsin \left(\frac{1}{C} \frac{\partial u_i}{\partial x_j} \right). \tag{2}$$

where μ, ρ and I have their usual meanings. Moreover, β and C are the parameters of the material fluid.

$$\begin{cases} \arcsin \left(\frac{1}{C} \frac{\partial u_i}{\partial x_j} \right) \cong \left(\frac{1}{C} \frac{\partial u_i}{\partial x_j} \right) - \frac{1}{6} \left(\frac{1}{C} \frac{\partial u_i}{\partial x_j} \right)^3, \\ \left| \frac{1}{C} \frac{\partial u_i}{\partial x_j} \right| \ll 1. \end{cases} \tag{3}$$

The mass, momentum and energy equations based on the boundary layer approximations are written by

$$\frac{\partial u}{\partial r} + \frac{u}{r} + \frac{\partial w}{\partial z} = 0. \tag{4}$$

$$u \frac{\partial u}{\partial r} + w \frac{\partial u}{\partial z} = \left(v + \frac{1}{\rho\beta C} \right) \frac{\partial^2 u}{\partial z^2} - \frac{1}{2\rho\beta C^3} \left(\frac{\partial u}{\partial z} \right)^2 \frac{\partial^2 u}{\partial z^2} - \frac{\sigma B^2(x)}{\rho} u. \tag{5}$$

$$u \frac{\partial T}{\partial r} + w \frac{\partial T}{\partial z} = \alpha \frac{\partial^2 T}{\partial z^2}. \tag{6}$$

Conditions for the momentum and thermal boundary are

$$\begin{cases} u = u_w + L \left(\frac{\partial u}{\partial z} \right) = ar + L \left(\frac{\partial u}{\partial z} \right), w = 0, T = T_w + k_1 \left(\frac{\partial T}{\partial z} \right), z = 0, \\ u \rightarrow 0, T \rightarrow T_\infty, z \rightarrow \infty. \end{cases} \tag{7}$$

In the above equation u and w are the velocity components in radial and axial directions respectively, u_w is the velocity at the wall, σ is the electrical conductivity, a is a constant with dimensional associated with radially stretching sheet rate, L is the velocity slip factor, and k_1 is the thermal slip factor, $\alpha \left(= \frac{k}{\rho c_p} \right)$ is the thermal diffusivity, k, c_p have their usual meanings.

By considering the variables defined below:

$$\begin{cases} u(r, z) = ar f'(\eta), w(r, z) = -\sqrt{av} f(\eta), \\ \theta(\eta) = \frac{T - T_\infty}{T_w - T_\infty}, \eta = \sqrt{\frac{a}{v}} z. \end{cases} \quad (8)$$

Equations (5),(6) are become as due to the conservation of momentum and energy laws,

$$(1 + \epsilon) f''' + 2f f'' - f'^2 - \epsilon \delta f''^2 f''' - M f' = 0. \quad (9)$$

$$\theta'' + 2Pr f \theta' = 0. \quad (10)$$

$$f(0) = 0, f'(0) = 1 + \alpha_1 f''(0), f'(\infty) = 0. \quad (11)$$

$$\theta(0) = 1 + \alpha_2 \theta'(0), \theta(\infty) = 0. \quad (12)$$

where M is the magnetic parameter and ϵ and δ are the fluid parameters. α_1 is the velocity slip parameter and α_2 is the thermal slip parameter. They are given as follows

$$M = \frac{\sigma B_0^2}{\rho a}, Pr = \frac{v}{\alpha}, \epsilon = \frac{1}{\mu \beta C}, \delta = \frac{u_w^3}{2rvC^2}, \alpha_1 = L\sqrt{\frac{a}{v}}, \alpha_2 = k_1\sqrt{\frac{a}{v}}. \quad (13)$$

The skin friction coefficient C_f is given by

$$C_f = \frac{\tau_w}{\frac{1}{2}\rho(u_w)^2} = \frac{\tau_{rz}|_{z=0}}{\frac{1}{2}\rho(u_w)^2} = Re_r \frac{-1}{2} \left((1 + \epsilon) f''(0) - \frac{\epsilon}{3} \delta f'''^3(0) \right). \quad (14)$$

Formula for the local Nusselt number can be written as follows

$$Nu_r = \frac{rq_w}{k(T_f - T_\infty)}, q_w = -k \frac{\partial T}{\partial z} |_{z=0}, Nu_r Re_r \frac{-1}{2} = -\theta'(0). \quad (15)$$

where $Re_r = \frac{u_w r}{v}$ is the Reynolds number.

3. Solution of the Problem:

SRM is in use to solve equations (10)- (12); see also Motsa and Makukula (2013). Spectral methods are favored here on account of their astoundingly high accuracy ,simplicity of execution in discretizing. The algorithm Spectral Relaxation Method is used to obtain the solution of similarity boundary layer problems with exponentially decay profiles. Chebyshev spectral collocation methods are used to discretize the differential equations (see, for example, in Canuto et al. (1988)and Trefethene (2000)).To get the ample accuracy of SRM we consider the number of grid points are 100 all the way through numerical experimentation is that $\eta_\infty = 20$. With regards to the SRM iteration scheme depicted above, equations (10)-(12) become

$$f'_{r+1} = P_{r+1}, f_{r+1}(0) = 0. \tag{16}$$

$$(1 + \epsilon - \epsilon\delta P_r'^2) P_{r+1}'' + 2(f_r)P_{r+1}' - MP_{r+1} = P_{r+1}^2. \tag{17}$$

$$\theta_{r+1}'' + (2Prf_r)\theta_{r+1}' = 0. \tag{18}$$

Following are considered as the boundary conditions to the above stated tactical approach of approximation method

$$P_{r+1}(0) = 1 + P'_{r+1}(0), \theta_{r+1}(0) = 1 + \theta'_{r+1}(0). \tag{19}$$

$$P_{r+1}(\infty) = 0, \theta_{r+1}(\infty) = 0. \tag{20}$$

The computational space of the domain $[0, L]$ is changed to the interim $[-1, 1]$ in Chebyshev spectral collocation method utilizing $\eta = L(\xi + 1)/2$ on which the spectral technique is actualized. Here L invokes the infinity boundary conditions. In spectral method the purpose of introducing \mathcal{D} where \mathcal{D} is the differentiation matrix, is to estimate the unknown variables and its derivatives at the collocation points. The following representation is the matrix vector product

$$\frac{\partial f_{r+1}}{\partial \eta} = \sum_{k=0}^{\bar{N}} D_{lk} f_r(\xi_k) = Df_r, l = 0, 1, 2 \dots \bar{N}. \tag{21}$$

The grid points are denoted with $\bar{N} + 1$ and the powers of D represent the higher-order derivatives, i.e.

$$f_r^{(p)} = D^p f_r. \tag{22}$$

The order of the derivative is represents with p , equations (16) - (20) are as follows after applying the spectral method

$$A_1 f_{r+1} = B_1, f_{r+1}(\xi_{\bar{N}}) = 0. \tag{23}$$

$$A_2 P_{r+1} = B_2, \sum_{k=0}^{\bar{N}} D_{\bar{N}k} P_{r+1}(\xi_k) - P_{r+1}(\xi_{\bar{N}}) = -1, P_{r+1}(\xi_0) = 0. \tag{24}$$

$$A_3 \theta_{r+1} = B_3, \sum_{k=0}^{\bar{N}} D_{\bar{N}k} \theta_{r+1}(\xi_k) - \theta_{r+1}(\xi_{\bar{N}}) = -1, \theta_{r+1}(\xi_0) = 0. \tag{25}$$

Here,

$$A_1 = D, B_1 = P_{r+1}. \tag{26}$$

$$A_2 = (1 + \epsilon - \epsilon \delta P_r^2) D^2 + \text{diag}(2f_r) D - MI, B_2 = P_{r+1}^2. \tag{27}$$

$$A_3 = D^2 + 2Pr \text{diag}(f_r) D, B_3 = 0. \tag{28}$$

In equations (26)-(28) I is an identity matrix and $\text{diag}[\]$ is a diagonal matrix, the sizes of all $(\bar{N} + 1) \times (\bar{N} + 1)$, the evaluation at the grid points then the functional values of f, P, θ are the f, P, θ respectively and the subscript r is used to represents the approximation numeral.

To start the SRM the initial guesses for equations (19)-(20) are as follows

$$f_0(\eta) = \left(\frac{1}{1 + \alpha_1} \right) (1 - e^{-\eta}), P_0(\eta) = \frac{1}{1 + \alpha_1} e^{-\eta}, \theta_0(\eta) = \frac{1}{1 + \alpha_2} e^{-\eta}. \tag{29}$$

Every one of these functions is chosen at random and satisfies the boundary conditions. The emphasis is reshaped until the point that joining is accomplished. In terms of infinity norm of spectral relaxation method by convergence is explained by

$$Er = Max(\|f_{r+1} - f_r\|, \|p_{r+1} - p_r\|, \|\theta_{r+1} - \theta_r\|). \quad (30)$$

To achieve the accuracy of the scheme no. of grid points are increased till the solutions are remains consistent and the fore coming increases cannot change the value of the solutions. The rate of convergence of the proposed SRM calculation can be enhanced essentially by applying the successive over-relaxation (SOR) technique to equations (23)-(25). To modify the SRM scheme ω is introduced where ω is a convergence controlling relaxation parameter in the SOR framework, for finding X is given by

$$AX_{r+1} = (1 - \omega)AX_r + \omega B. \quad (31)$$

Here we considered the convergence controlling relaxation parameter ω as less than unity i.e. ($\omega < 1$) to discuss the outcomes in the coming sections, applying the successive over-relaxation method is significantly improves the effectiveness and accuracy of the spectral relaxation method.

4. Results and Discussion

The MHD axisymmetric slip flow of Powell-Eyring flow over a radially stretching surface has been investigated through spectral relaxation method algorithm (9)-(12). The results of SRM were compared with those of MAT LAB bvp4c solver and given in tables 1- 4 which show a decent understanding between the two proposed techniques, this comparison gives a benchmark to gauge the precision and effectiveness of the technique.

The velocity of Powell-Eyring fluid is greater than the Newtonian model as shown in Figure 2. The reason is that the decrement of viscosity of Powell-Eyring fluid with shear rate due to this fluid velocity is accelerated.

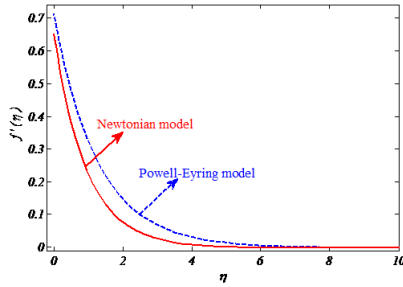


Figure 2: Graph for SRM solutions for comparison of Newtonian model vs. Powell - Eyring model.

From the Figure 3, it can be noticed that the velocity profile shows an increment with increase in ϵ . Whereas, temperature profiles decreases with increasing ϵ , as shown in the Figure 4. This is due to the viscosity of a shear thinning fluid decreases with an increase in ϵ . So fluid molecules flow with higher velocities, because of frictional force it is found that less heat is formed. From the above observations it is cleared that there is a decrease in the temperature distribution.

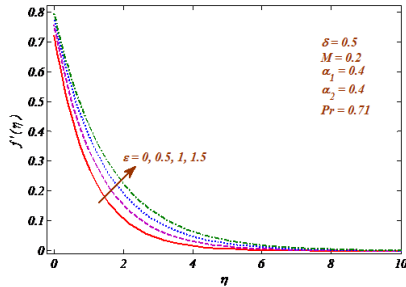


Figure 3: Graph for velocity profiles for various values of ϵ

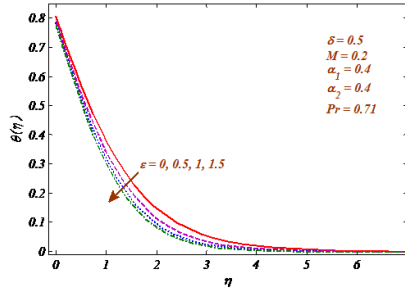


Figure 4: Graph for temperature profile for various values of ϵ .

Figure 5 portrays velocity field for varied values of magnetic parameter M and slip parameter α_1 . It can be clear that velocity profiles reduces with an enhancement in magnetic parameter M , physically, presented results occurs in the conductivity fluid and create a resistive type force i.e. Lorenz force on the fluid in the boundary layer because of this velocity of the fluid is reduces.

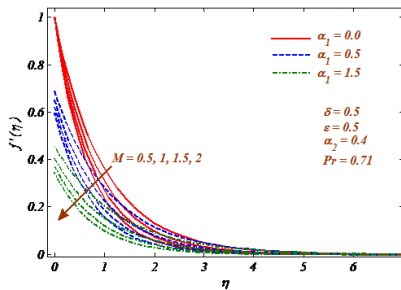


Figure 5: Graph for velocity profiles for various values of M & α_1 .

Clearly it is observed that the fluid velocity nearby a solid surface is equivalent to the velocity of the stretching sheet in the no-slip condition case i.e. $f'(0) = 1$ the thickness of the momentum boundary layer has been decreased by the increase of momentum slip parameter. This happens in light of the fact that the pumping of the stretching wall can be to some part transmitted to the fluid under slip condition. It is pointed out that α_1 is having a considerable impact on the solutions obtained.

The behaviour of magnetic parameter M and thermal slip parameter α_2 on the temperature distribution is shown in Figure 6. Temperature profiles show increasing behaviour for higher values of M , whereas decreasing behaviour for

α_2 . An increment in M produces higher Lorentz force (resistive force) which has the characteristic to convert some thermal energy into heat energy. Therefore the temperature profile increases. From the Figure 7, it is noticed that the decreasing heat transfer profiles for an increasing values of Pr it is because of the low thermal conductivity and in this manner heat can diffuse far from the heated sheet more rapidly. Henceforth, on account of increasing values of Prandtl number the boundary layer goes thinner and the heat transfer is reduced.

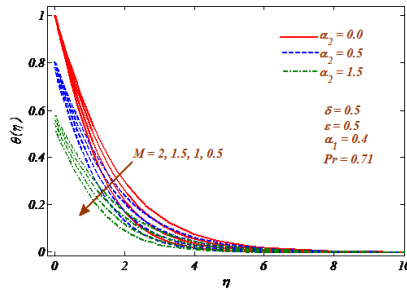


Figure 6: Graph for temperature profile for various values of M & α_2 .

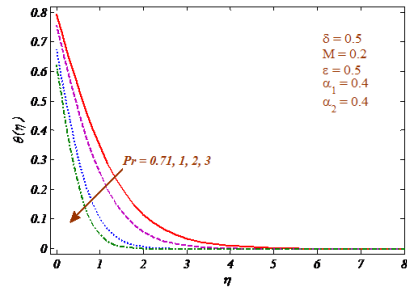


Figure 7: Graph for temperature profiles for various values of Pr

Table 1 and Table 2 displays the similarities between the coefficient of skin friction and local Nusselt number based on with the earlier studies. It concludes that there is a reasonable relation between them. From Table 1, it has noticed that skin friction coefficient rises with rise in ϵ , it decrease with an increase in δ . From Table 2 clearly, the observation is that the value of local Nusselt number is enhanced by enhancing the prandtl number. This is because of a fluid with higher Prandtl number gains high heat capacity and henceforth escalates the heat exchange. From Table 3, it is clear that skin friction coefficient increasing

function of \mathbf{M} but decreasing function of α_1 , The wall heat rate diminishes with an increase in \mathbf{M} & δ where as it rises with an increase in ϵ this is shown in Table 4. In evidence that the local Nusselt number partial thermal slip coefficient α_2 are found inversely. These results are alike to the previous findings by Zheng et al. (2013).

Tables 3 and 4 also give a comparison of the basic SRM and the SOR - accelerated SRM (with ω) for the number of iterations each method takes to yield eight decimal digit accurate results. The SRM results with relation are validated against those obtained by the bvp4c. These results are in excellent agreement for up to eight decimal digit accurate results. It can be seen that for small values of \mathbf{M} converges of basic SRM is slow. In this case introducing ω is seen to have the beneficial effect of significantly reducing the number of iterations required to give the desired accuracy.

Table 1: Comparison of coefficient of Skin-friction $C_f Re^{1/2}$ for various values of ϵ & δ when $M = \alpha_1 = \alpha_2 = 0$.

$C_f Re^{1/2}$			
ϵ	δ	Present study	[Hayat et al. (2016) (HAM)]
0.1	1.0	1.21541935	1.21542
0.2	1.0	1.25742284	1.25742
0.3	1.0	1.29957015	1.29957
0.1	2.0	1.19816228	1.19816
0.1	3.0	1.17851323	1.17851

Table 2: Comparison of rate of wall heat transfer $-\theta'(0)$ for various values of Pr when $\epsilon = \delta = M = \alpha_1 = \alpha_2 = 0$.

$-\theta'(0)$			
Pr	Present study	[Hayat et al. (2016) (HAM)]	[Wang (2007) (RK)]
0.2	0.25165169	0.25165	0.25167
0.7	0.66725733	0.66726	0.66729
2.0	1.32390437	1.32391	1.32391
7.0	2.72296754	2.72297	2.72299

Table 3: Numerical data of $-C_f Re^{1/2}$ for different parameters of involved parameters \mathbf{M} and α_1 when $\epsilon = 0.1, \delta = 1, \alpha_2 = 0.1, \& Pr = 0.71$.

\mathbf{M}	α_1	Basic SRM			SRM with SOR		Bvp4c
		iter	$-C_f Re^{1/2}$	ω	iter	$-C_f Re^{1/2}$	$-C_f Re^{1/2}$
0.5	0.1	30	1.10133147	0.85	15	1.10133147	1.10133147
1.0		29	1.25288115	0.9	13	1.25288115	1.25288115
1.5		16	1.38053336	0.9	13	1.38053336	1.38053336
2.0		14	1.49116553	0.95	10	1.49116553	1.49116553
	0.5	33	0.74057840	0.85	16	0.74057840	0.74057840
	1.0	33	0.53571924	0.85	16	0.53571924	0.53571924
	1.5	32	0.42288718	0.85	15	0.42288718	0.42288718
	2.0	29	0.35057475	0.85	15	0.35057475	0.35057475

Table 4: Numerical values of $Nu_r Re^{-1/2}$ for different parameters of involved parameters $\mathbf{M}, \epsilon, \delta$ & α_2 when $\alpha_1 = 0.1$ & $Pr = 0.71$.

\mathbf{M}	ϵ	δ	α_2	iter	Basic SRM		iter	SRM with SOR	
					$Nu_r Re^{-1/2}$	ω		$Nu_r Re^{-1/2}$	$Nu_r Re^{-1/2}$
0.5	0.1	1.0	0.1	30	0.61435961	0.85	15	0.61435961	0.61435961
1.0				29	0.57421372	0.9	13	0.57421372	0.57421372
1.5				16	0.54005650	0.9	13	0.54005650	0.54005650
2.0				14	0.51035543	0.95	10	0.51035543	0.51035543
	0.2			29	0.62241774	0.85	15	0.62241774	0.62241774
	0.3			28	0.62993299	0.85	15	0.62993299	0.62993299
	0.4			28	0.63695596	0.85	15	0.63695596	0.63695596
	0.5			27	0.64352940	0.85	15	0.64352940	0.64352940
		2.0		28	0.61116257	0.85	15	0.61116257	0.61116257
		3.0		27	0.60754866	0.85	15	0.60754866	0.60754866
		4.0		24	0.60332791	0.9	14	0.60332791	0.60332791
		5.0		22	0.59806873	0.9	17	0.59806873	0.59806873
			0.5	30	0.49316688	0.85	15	0.49316688	0.49316688
			1.0	30	0.39561482	0.85	15	0.39561482	0.39561482
			1.5	30	0.33028249	0.85	15	0.33028249	0.33028249
			2.0	30	0.28346992	0.85	15	0.28346992	0.28346992

5. Conclusions

The main results of present analysis are listed below.

1. The Powell-Eyring fluid is compared with Newtonian model and observed to have more velocity than that of Newtonian model.

2. **There is a decrease in the velocity and temperature by increasing corresponding slip parameters.**

3. The coefficient of skin friction is an increasing function of \mathbf{M} but a decreasing function of velocity slip parameter α_1 .

4. The rate of skin friction increases with ϵ and decreases with δ .

5. The wall heat rate diminishes with an increase in \mathbf{M} & δ where as it rises with an increase in ϵ .

6. The heat transfer rate **decreases** with an increase in pr & ϵ .

7. The fluid velocity nearby a solid surface is equivalent to the velocity of the stretching sheet in the no-slip condition case i.e. $f'(0) = 1$ the thickness of the momentum boundary layer has been decreased by the increase of momentum slip parameter

By applying the successive over-relaxation method is significantly improves

the effectiveness and accuracy of the spectral relaxation method. Our outcomes demonstrate that the spectral relaxation method is efficient and adequately powerful for use of solving fluid flow problems.

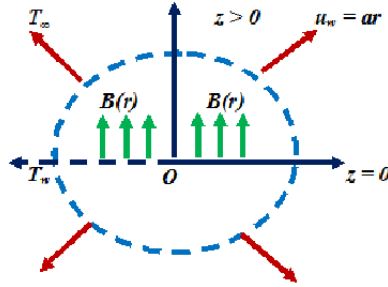


Figure 8: Schematic diagram .

Acknowledgement

We sincerely thank the anonymous referees for their valuable suggestions those are definitely improved the content of this paper.

Nomenclature

c_p - Specific heat under pressure maintained at constant level (J/kg K)

f - Non-dimensional stream function

u - **velocity component along radial(r) direction (m/s)**

w - **velocity component along axial(z) direction (m/s)**

T - Temperature of the fluid (0C)

T_w - Stretching surface's temperature

T_∞ - Ambient temperature of the fluid

u_w - In **radial(r)** direction stretching velocity

v_w - In **axial(z)** direction stretching velocity

B_0 - Magnetic field strength

k_p - Permeability

i - Time index during navigation

L - Scale

t - Time

I - is the identity tensor

\bar{N} - Number of grid points

Pr - Prandtl number

V - Velocity vector

Re_r - **Local Reynolds number**

C_{fr} - **skin friction coefficient along radial(r) direction**

C_{fz} - **skin friction coefficient along axial(z) direction**

Nu_r - **Local Nusselt number**

q_w - Heat flux of the surface

Greek symbols

k - Thermal conductivity (W/m K)

μ - Thermal viscosity (N s/m)

ρ - Fluid density (kg/m³)

τ_{wr} - In radial direction wall shear stress

τ_{wz} - In axial direction wall shear stress

$V = \mu/\rho$ - Kinematic viscosity

η - Similarity variable

$\bar{\tau}$ - Extra stress tensor

Γ - Time dependent material constant

θ - Temperature with dimensionless

Subscript

w - Surface condition

∞ - Infinity condition

Super script

' - Differentiation with respect to η

References

- Bilal Ashraf, M., Hayat, T., and Alsaedi, A. (2015). Three-dimensional flow of eyring-powell nanofluid by convectively heated exponentially stretching sheet. *The European Physical Journal Plus*, 130(5):111–129.
- Canuto, C., Hussaini, M. V., Quarteroni, A., and Zang, T. A. (1988). *Spectral Methods in Fluid Dynamics*. Springer Berlin.
- Hayat, T., Makhdoom, S., Awais, M., Saleem, S., and Rashidi, M. M. (2016). Axisymmetric powell-eyring fluid flow with convective boundary condition: optimal analysis. *Applied Mathematics and Mechanics*, 37(7):919–928.
- Ismail, N. S., Arifin, N. M., Nazar, R., and Bachok, N. (2019). Stability analysis of stagnation-point flow and heat transfer over an exponentially shrinking sheet with heat generation. *Malaysian Journal of Mathematical Sciences*, 13(2):107–122.
- Jaina, S. and Choudhary, R. (2015). Effects of mhd on boundary layer flow in porous medium due to exponentially shrinking sheet with slip. *Procedia Engineering*, 127:1203 – 1210.
- Javed, T., Ali, N., Abbas, Z., and Sajid, M. (2013). Flow of an eyring-powell non-newtonian fluid over a stretching sheet. *Chemical Engineering Communications*, 200:327–336.
- Khalil-Ur-Rehman, Khan, A. A., Malik, M., and Makinde, O. (2017a). Thermo-physical aspects of stagnation point magnetonanofluid flow yields by an inclined stretching cylindrical surface: a non-newtonian fluid model. *Journal of*

the Brazilian Society of Mechanical Sciences and Engineering, 39,no.9:3669–3682.

- Khalil-Ur-Rehman, Malik, A. A., Malik, M., and Tahir, M. I. Z. (2018). On new scaling group of transformation for prandtl-eyring fluid model with both heat and mass transfer. *Results in Physics*, 8:552–558.
- Khalil-Ur-Rehman, Malik, M., Bilal, S., and Bibi, M. (2017b). Numerical analysis for mhd thermal and solutal stratified stagnation point flow of powell-eyring fluid induced by cylindrical surface with dual convection and heat generation effects. *Results in Physics*, 7:482–492.
- Khalil-Ur-Rehman, Malik, M., Bilal, S., Bibi, M., and Ali, U. (2017c). Logarithmic and parabolic curve fitting analysis of dual stratified stagnation point mhd mixed convection flow of eyring-powell fluid induced by an inclined cylindrical stretching surface. *Results in Physics*, 7:544–552.
- Khalil-Ur-Rehman, Saba, N. U., and Malik, M. A. A. M. (2017d). Encountering heat and mass transfer mechanisms simultaneously in powell-eyring fluid through lie symmetry approach. *Case studies in thermal engineering*, 10:541–549.
- Mansur, S., Ishak, A., and Pop, I. (2014). Flow and heat transfer of nanofluid past stretching/shrinking sheet with partial slip boundary conditions. *Applied Mathematics and Mechanics*, 35:1401–1410.
- McCormack, P. D. and Crane, L. J. (1973). *Physical Fluid Dynamics*. Academic Press.
- Motsa, S. and Makukula, Z. (2013). On spectral relaxation method approach for steady von karman flow of a reiner-rivlin fluid with joule heating, viscous dissipation and suction/injection. *Central European Journal of Physics*, 11:363–374.
- Shaw, S., Kameswaran, P. K., and Sibanda, P. (2016). Effects of slip on non-linear convection in nanofluid flow on stretching surfaces. *Boundary Value Problems*, 2:207–243.
- Trefethene, L. N. (2000). *Spectral Methods in MATLAB*. SIAM Philadelphia.
- Wang, C. Y. (2007). Natural convection on a vertical radially stretching sheet. *Journal of Mathematical Analysis and Applications*, 332:877–883.
- Yoshimura, A. and Prudhomme, R. K. (1998). Wall slips corrections for couette and parallel disc viscometers. *Journal of Rheology*, 32:53–67.

Subba Rao, M. V., Gangadhar, K. & Varma, P. L. N.

Zheng, L., Zhang, C., Zhang, X., and Zhang, J. (2013). Flow and radiation heat transfer of a nanofluid over a stretching sheet with velocity slip and temperature jump in porous medium. *J. Franklin Inst.*, 350:990–1007.